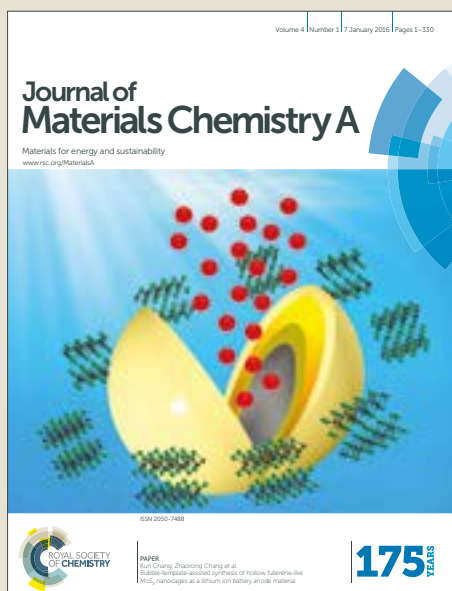


# Journal of Materials Chemistry A

Accepted Manuscript



This article can be cited before page numbers have been issued, to do this please use: F. Xiao, H. Xu, Q. Wu, Y. Chu, J. Jiang, L. Zhang, S. Pan, C. Zhang, L. Zhu, F. Deng, X. Meng, S. Maurer, R. McGuire, A. Parvulescu and U. Mueller, *J. Mater. Chem. A*, 2018, DOI: 10.1039/C8TA01734D.



This is an Accepted Manuscript, which has been through the Royal Society of Chemistry peer review process and has been accepted for publication.

Accepted Manuscripts are published online shortly after acceptance, before technical editing, formatting and proof reading. Using this free service, authors can make their results available to the community, in citable form, before we publish the edited article. We will replace this Accepted Manuscript with the edited and formatted Advance Article as soon as it is available.

You can find more information about Accepted Manuscripts in the [author guidelines](#).

Please note that technical editing may introduce minor changes to the text and/or graphics, which may alter content. The journal's standard [Terms & Conditions](#) and the ethical guidelines, outlined in our [author and reviewer resource centre](#), still apply. In no event shall the Royal Society of Chemistry be held responsible for any errors or omissions in this Accepted Manuscript or any consequences arising from the use of any information it contains.



Journal Name

ARTICLE

## Efficient synthesis of aluminosilicate RTH zeolite with good catalytic performances in NH<sub>3</sub>-SCR and MTO reactions

Hao Xu,<sup>a</sup> Qinming Wu,<sup>\*,a</sup> Yueying Chu,<sup>b</sup> Jingang Jiang,<sup>c</sup> Ling Zhang,<sup>a</sup> Shuxiang Pan,<sup>a</sup> Changsheng Zhang,<sup>a</sup> Longfeng Zhu,<sup>a,d</sup> Feng Deng,<sup>b</sup> Xiangju Meng,<sup>a</sup> Stefan Maurer,<sup>e</sup> Robert McGuire,<sup>f</sup> Andrei-Nicolae Parvulescu,<sup>f</sup> Ulrich Müller<sup>f</sup> and Feng-Shou Xiao<sup>\*,a</sup>

Received 00th January 20xx,  
Accepted 00th January 20xx

DOI: 10.1039/x0xx00000x

www.rsc.org/

2,6-methyl-N-methylpyridinium, as a novel organic template, is employed for synthesis of RTH aluminosilicate zeolite with a SiO<sub>2</sub>/Al<sub>2</sub>O<sub>3</sub> ratio of 17.6. The amount of 2,6-methyl-N-methylpyridinium template, the Na<sub>2</sub>O/SiO<sub>2</sub> ratio, the SiO<sub>2</sub>/Al<sub>2</sub>O<sub>3</sub> ratio, and the H<sub>2</sub>O/SiO<sub>2</sub> ratio in the starting gel significantly influence the crystallization of RTH zeolite. Several analytical methods such as XRD, SEM, N<sub>2</sub> sorption, TG-DTA, DRIFT and NMR were employed for characterisation of the obtained RTH zeolites and to understand the crystallization process with the new template. Very interestingly, the crystallization of RTH zeolite with the new template takes very short time (12 h at 130 °C and 50 min at 240 °C) compared with conventional RTH zeolites synthesis reported in the literature (72 h at 130 °C). Theoretical calculations show that this novel organic template has lower interaction energies for the zeolite cage space filling than that of the previous organic templates in the literatures, which lead to the stronger structural directing. Kinetic results show that the activation energy of this novel organic template is much lower than the traditional one. Catalytic tests show that copper exchanged RTH zeolite (Cu-RTH) exhibits good catalytic properties in the NH<sub>3</sub>-SCR reaction and H-RTH zeolite catalyst has excellent selectivities for ethylene and propylene in MTO reaction.

### Introduction

Zeolites, microporous silica-based and aluminophosphate-based crystalline materials, have been widely used as catalysts in the industrial processes of oil refining and chemical production due to their high surface area, large pore volume, uniform accessible microporous channels, and excellent thermal and hydrothermal stabilities.<sup>1</sup> For example, aluminosilicate Y zeolite is applied for fluid catalytic cracking, and aluminosilicate ZSM-5 zeolite is successful used for shape-selective catalytic synthesis of p-xylene.<sup>2</sup> Recently, small-pore zeolites with pore openings limited by 8-membered rings in

tetrahedral coordination, have received noticeable attention due to their outstanding performance in selective catalytic reduction of NO<sub>x</sub> with NH<sub>3</sub> (NH<sub>3</sub>-SCR) and methanol-to-olefin (MTO) reactions. Examples include SAPO-34 and SSZ-13, which show excellent MTO and NH<sub>3</sub>-SCR performances, respectively.<sup>3</sup>

The RTH-type zeolite discovered in 1995, are promising candidates for the aforementioned catalytic applications due to the particular two-dimensional 8 MR pore structure (aperture size of 4.1×3.8 Å and 5.6×2.5 Å). RTH zeolite was first synthesized as borosilicate in the presence of 1,2,2,6,6-pentamethylpiperidine as organic template, and denoted as RUB-13.<sup>4</sup> Later, the aluminosilicate RTH designated as SSZ-50 was successfully prepared by using N-ethyl-N-methyl-5,7,7-trimethyl-azonium bicyclo [4.1.1] octane cation.<sup>5</sup> It is worth noting that the synthesis of above organic templates is very complex due to the multistep synthesis methods, which strongly hinders its large scale synthesis. Recently, a facile method for synthesizing aluminosilicate RTH in the presence of a series of novel imidazolium cations has been reported.<sup>6</sup>

Despite the encouraging progress achieved in RTH zeolite synthesis in recent years, the crystallization of RTH zeolite is still very slow, which impacts its further application.<sup>4-7</sup> Therefore, it is strongly desirable to shorten the crystallization time of RTH zeolite.

Our group previously reported that the high silica Y zeolite with excellent properties could be successfully synthesized in the presence of N-methylpyridinium iodide.<sup>8</sup> Furthermore, we have

<sup>a</sup> Key Laboratory of Applied Chemistry of Zhejiang Province, Zhejiang University, Hangzhou 310028, China. E-mail: qinmingwu@zju.edu.cn, fsxiao@zju.edu.cn.

<sup>b</sup> State Key Laboratory of Magnetic Resonance and Atomic and Molecular Physics, Wuhan Center for Magnetic Resonance, Wuhan Institute of Physics and Mathematics, Wuhan 430071, China.

<sup>c</sup> Shanghai Key Laboratory of Green Chemistry and Chemical Processes, School of Chemistry and Molecular Engineering, East China Normal University, Shanghai 200062, China.

<sup>d</sup> College of Biological, Chemical Sciences and Engineering, Jiaying University, Jiaxing 314001, China.

<sup>e</sup> BASF Catalysts (Shanghai) Co., Ltd., 239 Luqiao Road, Jinqiao Export Process Zone Pudong New District, Shanghai 201206, China.

<sup>f</sup> BASF SE, GCC/PZ-M311, Ludwigshafen 67056, Germany.

Electronic Supplementary Information (ESI) available: Extended characterization details, TG-DTA Curves, XRD patterns, SEM images, DRIFT spectra, NMR spectra, NH<sub>3</sub>-TPD curves, MTO reaction curves, porosity data and the dependence of the crystallinity on crystallization time. See DOI: 10.1039/x0xx00000x

## ARTICLE

## Journal Name

made theoretical calculations to check the pyridyl cation for synthesizing RTH zeolite. Very interestingly, the interaction energy between 2,6-methyl-N-methylpyridinium cation and RTH zeolite is lower than the energies of the conventional organic template (polymethylated [4.1.1] octanes) and the newly developed organic template (1,2,3-trimethylimidazolium) reported in the literature.<sup>5,6</sup> Therefore, 2,6-methyl-N-methylpyridinium cation as organic template could be suitable for synthesizing RTH zeolite.

It is consistent with the expectation that the observed experimental results agree well with the results of the predicted interaction energies. More importantly, the aluminosilicate RTH zeolite would be obtained at very short crystallization time (12 h at 130 °C and 50 min at 240 °C). In addition, Cu-RTH zeolite exhibits good catalytic property in NH<sub>3</sub>-SCR reaction, and H-RTH zeolite displays excellent selectivity for light olefins in MTO reaction.

## Experimental

### Computational Method

The location and amount of the organic structure directing agent (OSDA) within the RTH framework were studied by molecular mechanics simulations using the sorption program in Materials Studio 7.0 software. The CVFF force field was selected for the calculation, and the most stable locations for the OSDA molecules were obtained by sorption program. The zeolite framework was assumed to be pure silicate, due to the distribution of the Al atoms in the framework is not clear. The geometry of the OSDA molecules and the RTH zeolite was first optimized using the CVFF force field and allowed to change for the locate calculation.

Based on the simulation structures, the OSDAs in RTH zeolite are further optimized by Dmol3 program, with the generalized gradient approximation (GGA) proposed by Perdew-Burke-Ernzerhof (PBE) functional. The ultrasoft pseudopotential, medium planewave cut-off energy and a default medium level Monkhorst-Pack K-point (1×1×1) were adopted to sample the Brillouin zone. DFT-D method was used in the structure optimization to accurately describe the weak interaction in the zeolite. During the calculation, the OSDAs are allowed to relax while the unit cell and the framework atoms were fixed. On the basis of the DFT calculational result, the interaction energy was calculated as the energy difference between the zeolite adsorption complex and the sum of the OSDAs and zeolite. *i.e.*,  $E_{\text{int}} = E_{\text{zeolite-OSDAs}} - E_{\text{zeolite}} - E_{\text{OSDAs}}$ .

### Materials

Y zeolite (Si/Al = 6, 12) provided by BASF, sodium metaaluminate (NaAlO<sub>2</sub>, AR, 99%, Sinopharm Chemical Reagent Co., Ltd.), sodium hydroxide (NaOH, AR, 96%, Sinopharm Chemical Reagent Co., Ltd.), 2,6-dimethylpyridine (C<sub>7</sub>H<sub>9</sub>N, 98%, Aladdin Chemistry Co., Ltd.), 1,2-dimethylimidazole (C<sub>5</sub>H<sub>8</sub>N<sub>2</sub>, 98%, Aladdin Chemistry Co., Ltd.), iodomethane (CH<sub>3</sub>I, 99.5%, Sinopharm Chemical Reagent Co., Ltd.), ethanol (C<sub>2</sub>H<sub>6</sub>O, 99.7%, Sinopharm Chemical Reagent Co., Ltd.), diethyl ether (C<sub>4</sub>H<sub>10</sub>O, 99.5%, Sinopharm Chemical Reagent Co., Ltd.), colloidal silica (40 wt% SiO<sub>2</sub> in water, Sigma-

Aldrich Co.), tetrapropylammonium hydroxide solution (40% TPAOH in water, Sinopharm Chemical Reagent Co., Ltd.), anion-exchange resin (Tianjin Fuchen Chemical Reagents Factory), and ammonium nitrate (NH<sub>4</sub>NO<sub>3</sub>, AR, 99%, Beijing Chemical Reagent Co., Ltd.) were used without further purification. The deionized water was made in our laboratory.

### Synthesis

**Synthesis of OSDAs.** 2,6-methyl-N-methylpyridinium iodide was synthesized by dissolving 0.1 mol of 2,6-dimethylpyridine and 0.12 mol of iodomethane in 20 g of ethanol, then heating the mixture to 80 °C under stirring and keeping it under these conditions for 12 h in a dark place. The solvent and excess iodomethane were removed under rotary evaporation and the product was washed with ether. The molecular structure was verified using <sup>1</sup>H and <sup>13</sup>C nuclear magnetic resonance (NMR). The product was converted from the iodide to the hydroxide form (denoted as ROH) using an anion exchange resin.

1,2,3-trimethylimidazolium was synthesized by dissolving 0.1 mol of 1,2-dimethylimidazole and 0.1 mol of iodomethane in 20 g of ethanol, stirring at room temperature for 48 h in a dark place. The solvent and excess iodomethane were removed using rotary evaporation and the product was washed with ether. The structure was verified using <sup>1</sup>H and <sup>13</sup>C nuclear magnetic resonance (NMR). The product was converted from the iodide to the hydroxide form using an anion exchange resin.

**Synthesis of RTH zeolites.** A synthetic mixture with a molar composition of 0~0.36 ROH : 0~0.18 Na<sub>2</sub>O : 1.0 SiO<sub>2</sub> : 0.04 Al<sub>2</sub>O<sub>3</sub> : 18~85 H<sub>2</sub>O was prepared by mixing Y zeolite, ROH, sodium hydroxide, and deionized water. In a typical synthesis, 1 g of Y zeolite was mixed with 5.8 g of ROH solution (0.6 mol/L ROH) and stirred at room temperature for 2 h. Then, 0.15 g of NaOH was added. The synthesis mixture was stirred at room temperature for 2 h, transferred in a Teflon-lined autoclave oven and crystallized at 130 °C for 12 h. After filtrating, washing, drying, and calcining at 550 °C for 4 h, the product was finally obtained. The H-form of the sample (H-RTH) was prepared by ion-exchange with 1 M NH<sub>4</sub>NO<sub>3</sub> solution and calcination at 550 °C for 4 h. This ion-exchange procedure was repeated once. The Cu-form of the sample (Cu-RTH) was prepared by ion-exchange of the H-form RTH zeolite with 1 M CuAc<sub>2</sub> solution and calcination at 550 °C for 4 h.

By replacing OSDA to 1,2,3-trimethylimidazolium hydroxide, the comparative RTH zeolites were synthesized at 130 °C for 0~144 h.

**Synthesis of ZSM-5 zeolite.** A synthetic mixture with a molar composition of 0.30 TPAOH : 0.05 Na<sub>2</sub>O : 1.0 SiO<sub>2</sub> : 0.03 Al<sub>2</sub>O<sub>3</sub> : 20 H<sub>2</sub>O was prepared by mixing sodium metaaluminate, TPAOH solution (40% in water), colloidal silica (40% in water), and deionized water. The synthetic mixture was transferred in a Teflon-lined autoclave oven and crystallized at 180 °C for 72 h. After filtrating, washing, drying, and calcining at 550 °C for 4 h, the product was finally obtained. The H-form of the sample (H-ZSM-5) was prepared by ion-exchange with 1 M NH<sub>4</sub>NO<sub>3</sub>

solution and calcination at 550 °C for 4 h. This ion-exchange procedure was repeated once.

### Characterizations

X-ray powder diffraction (XRD) patterns were measured with a Rigaku Ultimate VI X-ray diffractometer (40 kV, 40 mA) using  $\text{Cu}_{\text{K}\alpha}$  ( $\lambda=1.5406 \text{ \AA}$ ) radiation. The  $\text{N}_2$  sorption isotherms at the temperature of liquid nitrogen were measured using Micromeritics ASAP 2020M and Tristar system. The sample composition was determined by inductively coupled plasma (ICP) with a Perkin-Elmer 3300DV emission spectrometer. Scanning electron microscopy (SEM) experiments were performed on Hitachi SU-1510 and SU-8010 electron microscopes.  $^{27}\text{Al}$ ,  $^{29}\text{Si}$ , and  $^{13}\text{C}$  MAS NMR spectra were recorded on a Varian Infinity Plus 400 spectrometer, and the chemical shifts were referenced to  $\text{Al}(\text{H}_2\text{O})_6^{3+}$ , tetramethylsilane and adamantane, respectively. The acidity of the catalysts was measured by the temperature-programmed-desorption of ammonia ( $\text{NH}_3$ -TPD). The catalyst was prepared at 450 °C in a He flow for 1 h, followed by the adsorption of  $\text{NH}_3$  at 100 °C for 1 h. After saturation, the catalyst was purged by He flow for 3 h to remove the physically adsorbed ammonia on the sample. Then, desorption of  $\text{NH}_3$  was carried out from 100 to 600 °C with a heating rate of 10 °C/min. The amount of  $\text{NH}_3$  desorbed from the sample was detected by a thermal conductivity detector. The diffuse reflectance infrared Fourier transform (DRIFT) spectra were recorded on a Bruker Tensor 27 *in situ* infrared spectrometer.

### Catalytic tests

Catalytic activities in selective catalytic reduction of ammonia ( $\text{NH}_3$ -SCR) were measured in a fixed-bed quartz reactor in a gaseous mixture containing 500 ppm of  $\text{NO}$ , 500 ppm of  $\text{NH}_3$ , 10% of  $\text{O}_2$ , and  $\text{N}_2$  as a balance gas. The gas hourly space velocity (GHSV) was 80 000  $\text{h}^{-1}$ .

Methanol-to-olefin (MTO) reactions were carried out in a fixed-bed reactor at atmospheric pressure. A total of 0.5 g of catalyst (20-40 mesh) was loaded into the reactor. The sample was pretreated in flowing nitrogen at 550 °C for 1 h, and then the temperature of the reactor was decreased to 480 °C or 400 °C.  $\text{CH}_3\text{OH}$  was pumped into the reactor under nitrogen. The weight hourly space velocity (WHSV) was 1.0  $\text{h}^{-1}$  or 2.0  $\text{h}^{-1}$ . The products were analyzed online by an Agilent 6890 gas chromatograph equipped with a FID detector and a HP-PONA methyl siloxane capillary column.

## Results and discussion

### Theoretical calculations

Results of the interaction energies interaction between the OSDA and the RTH structure are shown in Figure 1 and the calculated values are presented in Table 1. The conventional OSDA of polymethylated [4.1.1] octane cations<sup>5</sup> and the newly developed OSDA of 1,2,3-trimethylimidazolium cation<sup>6c</sup> were compared to the new designed organic template of 2,6-methyl-N-methylpyridinium cation. In these calculations, only two of the N-ethyl-N-methyl-

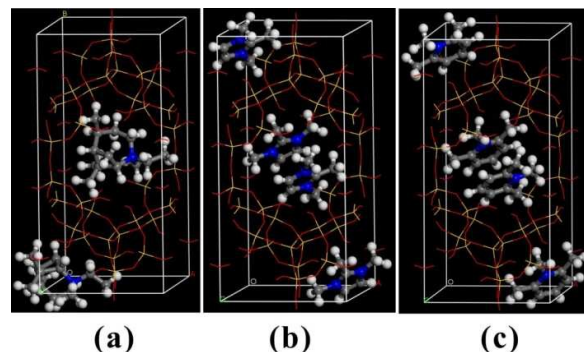


**Figure 1** Positions of OSDAs within the RTH framework for (a) N-ethyl-N-methyl-5,7,7-trimethyl-azonium bicyclo [4.1.1] octane cations, (b) 1,2,3-trimethylimidazolium cations and (c) 2,6-methyl-N-methylpyridinium cations.

5,7,7-trimethyl-azonium bicyclo [4.1.1] octane cations were fitting per unit cell. In contrast, as for 1,2,3-trimethylimidazolium cations and 2,6-methyl-N-methylpyridinium cations, four of these OSDA molecules were fitting per unit cell based on energy optimizations for the framework pore space filling.

The interaction energy between 2,6-methyl-N-methylpyridinium cation is lower than that of the other two OSDAs. This result indicates that 2,6-methyl-N-methylpyridinium cation is more suitable for synthesizing zeolite RTH.

### Sample characterization

Figure 2A shows XRD pattern of RTH zeolite synthesized in the presence of 2,6-methyl-N-methylpyridinium cation under static condition for 12 h at 130 °C, giving characteristic peaks associated with RTH structure. Figure 2B-a shows  $\text{N}_2$  sorption isotherms of as-synthesized RTH zeolite. Clearly, the sample has not any microporous adsorption, suggesting that the microporosity is fully filled with the OSDA. Thermal analysis (TG-DTA) of the as-synthesized RTH zeolite exhibits major exothermic peaks at 200-800 °C accompanied by a weight loss at about 22.4 %, which is related to the decomposition of the OSDA (Figure S1). After calcination at 550 °C for 4 h and ion-exchanging to H-form,  $\text{N}_2$  sorption isotherms of the sample (Figure 2B-b) shows typical Langmuir-type curve. A steep adsorption increase occurs in the curve at a relative pressure  $10^{-6} < P/P_0 < 0.01$ , which is due to the filling of micropores by  $\text{N}_2$ . Correspondingly, a BET surface area and micropore volume of 576  $\text{m}^2/\text{g}$  and 0.26  $\text{cm}^3/\text{g}$  were measured.

**Table 1** The calculated interaction energies (kcal/mol) between OSDAs and RTH zeolite.

| OSDAs | 1 OSDA<br>/cell | 2 OSDAs<br>/cell | 3 OSDAs<br>/cell | 4 OSDAs<br>/cell |
|-------|-----------------|------------------|------------------|------------------|
| a     | -95.5           | -205.3           | -                | -                |
| b     | -72.4           | -165.5           | -249.9           | -353.9           |
| c     | -77.1           | -168.3           | -259.4           | -360.7           |

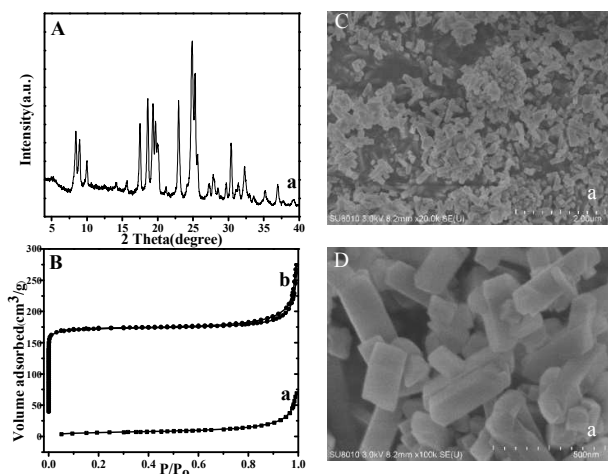


**Figure 2** (A) XRD pattern, (B)  $N_2$  sorption isotherms, (C) SEM image (scale bar 2  $\mu\text{m}$ ), and (D) SEM image (scale bar 500 nm) of (a) as-synthesized RTH zeolite, and (b) H-RTH zeolite.

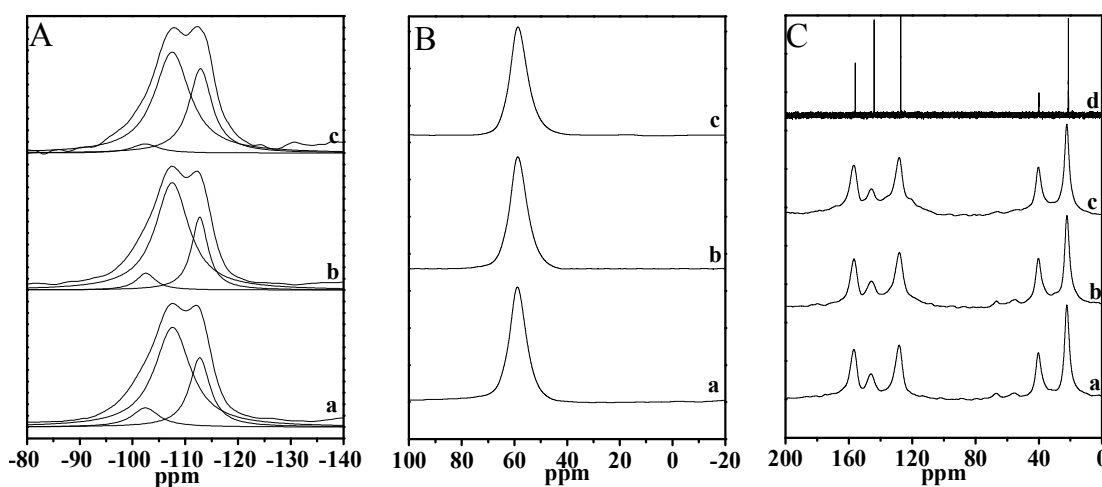
Figure 2C shows low magnification SEM image of as-synthesized RTH sample, giving very uniform crystal morphology, which indicates the high crystallinity of the product obtained. The high magnification SEM image (Figure 2D) of as-synthesized RTH sample exhibits that the particles are blocky (100–300 nm). ICP analysis shows that the  $\text{SiO}_2/\text{Al}_2\text{O}_3$  ratio in the product is about 17.6. RTH zeolite synthesized in the presence of 2,6-methyl-N-methylpyridinium cation at the temperature of 150  $^\circ\text{C}$ , 180  $^\circ\text{C}$ , and 240  $^\circ\text{C}$  are also well characterized by XRD patterns and SEM images (Figure S2).

Figure 3 shows  $^{29}\text{Si}$ ,  $^{27}\text{Al}$ , and  $^{13}\text{C}$  MAS NMR spectra of the as-synthesized RTH zeolites at the temperature of 130  $^\circ\text{C}$ , 180  $^\circ\text{C}$ , and 240  $^\circ\text{C}$ . Figure 3A shows the  $^{29}\text{Si}$  MAS NMR spectra of the as-synthesized RTH zeolites giving the peaks at about -112.2, -107.7 and -102.1 ppm. The peaks at -112.2 and -107.7 ppm are assigned to Si(4Si) species, while the peaks at -102.1 ppm are assigned to Si(3Si)OH species. Very interestingly, the signal intensity of

Si(3Si)OH species is of 9.3% at the synthesis temperature of 130  $^\circ\text{C}$ , while this signal intensity is of 6.3% and 4.2% at the synthesis temperature of 180  $^\circ\text{C}$  and 240  $^\circ\text{C}$ , respectively. Considering the same Si/Al ratios in the products, the lower intensity of Si(3Si)OH species means lower concentration of structural defects (Si-OH). Figure 3B shows the  $^{27}\text{Al}$  MAS NMR spectra of the as-synthesized RTH zeolites, showing a sharp band at 59 ppm associated with tetrahedrally coordinated aluminum species in the framework. The absence of a signal around zero ppm indicates that there is no extra framework Al species in the samples. Figure 3C compares the  $^{13}\text{C}$  MAS NMR spectra of the as-synthesized RTH zeolites with the liquid  $^{13}\text{C}$  NMR spectrum of 2,6-methyl-N-methylpyridinium iodide. Clearly, 2,6-methyl-N-methylpyridinium cations mostly exist in the channel of RTH zeolite obtained at the three crystallization temperatures. Figure S3 shows the DRIFT spectra of H-RTHs synthesized at 130  $^\circ\text{C}$ , 180  $^\circ\text{C}$  and 240  $^\circ\text{C}$ , respectively. Obviously, the H-RTH zeolite synthesized at higher temperature has lower concentration of structural defects (Si-OH). The BET surface areas and micropore volume of H-RTHs synthesized at 130  $^\circ\text{C}$ , 180  $^\circ\text{C}$  and 240  $^\circ\text{C}$  are presented in Table S1.

Table 2 presents effects of the synthesis conditions variation on the crystallization of the RTH zeolite. When NaOH is absent, the product is Y zeolite (Run 1, Table 2). When the  $\text{Na}_2\text{O}/\text{SiO}_2$  ratio is higher than 0.18, the product is mixed RTH zeolite with Y zeolite phase (Run 4, Table 2). When the organic template is absent, the product is amorphous (Run 5, Table 2). When the  $\text{ROH}/\text{SiO}_2$  ratio is 0.07, the sample is a mixture of RTH with Y zeolite (Run 6, Table 2). Increasing the  $\text{ROH}/\text{SiO}_2$  ratio to 0.14 results in a complete crystallization of RTH zeolite (Run 7, Table 2). Furthermore, the ratios of  $\text{H}_2\text{O}/\text{SiO}_2$  in the synthesis are carefully studied, and it is found that relatively high  $\text{H}_2\text{O}/\text{SiO}_2$  ratios (e.g. 85) result in incomplete crystallization (Run 11, Table 2). When the Y zeolite with Si/Al ratio at 6 was used, we cannot obtain RTH zeolite (Run 12–14, Table 2).

It is worth mentioning that the crystallization time for synthesis of RTH zeolite takes only 12 h at 130  $^\circ\text{C}$  in this work, which is very short compared with RTH zeolite reported in the



**Figure 3** (A)  $^{29}\text{Si}$ , (B)  $^{27}\text{Al}$ , and (C)  $^{13}\text{C}$  MAS NMR spectra of as-synthesized RTH zeolites at the temperature of (a) 130  $^\circ\text{C}$ , (b) 180  $^\circ\text{C}$  and (c) 240  $^\circ\text{C}$ . (d)  $^{13}\text{C}$  NMR spectrum in  $\text{D}_2\text{O}$  solution of 2,6-methyl-N-methylpyridinium cation.

## Journal Name

## ARTICLE

**Table 2** Impact of synthesis conditions on RTH zeolite crystallization

| Run <sup>a</sup> | Na <sub>2</sub> O/SiO <sub>2</sub> | ROH/SiO <sub>2</sub> | H <sub>2</sub> O/SiO <sub>2</sub> | Products <sup>b</sup> |
|------------------|------------------------------------|----------------------|-----------------------------------|-----------------------|
| 1                | 0                                  | 0.21                 | 18                                | Y                     |
| 2                | 0.04                               | 0.21                 | 18                                | RTH                   |
| 3                | 0.14                               | 0.21                 | 18                                | RTH                   |
| 4                | 0.18                               | 0.21                 | 18                                | Y+RTH                 |
| 5                | 0.11                               | 0                    | 18                                | Amor                  |
| 6                | 0.11                               | 0.07                 | 18                                | Y+RTH                 |
| 7                | 0.11                               | 0.14                 | 18                                | RTH                   |
| 8                | 0.11                               | 0.36                 | 18                                | RTH                   |
| 9                | 0.11                               | 0.21                 | 4.5                               | RTH                   |
| 10               | 0.11                               | 0.21                 | 45                                | RTH                   |
| 11               | 0.11                               | 0.21                 | 85                                | Y+RTH                 |
| 12               | 0.11                               | 0.07                 | 18                                | Y                     |
| 13               | 0.11                               | 0.11                 | 18                                | Y                     |
| 14               | 0.11                               | 0.14                 | 18                                | Y                     |
| 15 <sup>c</sup>  | 0.11                               | 0.21                 | 18                                | RTH                   |
| 16 <sup>c</sup>  | 0.11                               | 0.21                 | 18                                | RTH                   |

<sup>a</sup> Using Y zeolite (Si/Al = 12, run 1-11, 15-16; Si/Al = 6, run 12-14) as raw material.

<sup>b</sup> The phase appearing first is dominant.

<sup>c</sup> The samples were synthesized at 130 °C for 12 h (run 1-14), 180 °C for 3 h (run 15) and 240 °C for 50 min (run 16).

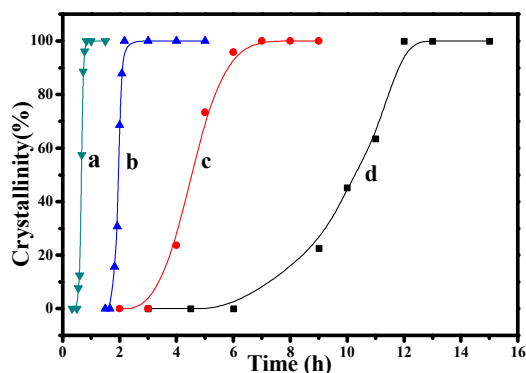


**Figure 4** The dependences of RTH zeolite crystallinity on crystallization time using 2,6-methyl-N-methylpyridinium cation as organic template at (a) 240 °C, (b) 180 °C, (c) 150 °C and (d) 130 °C.

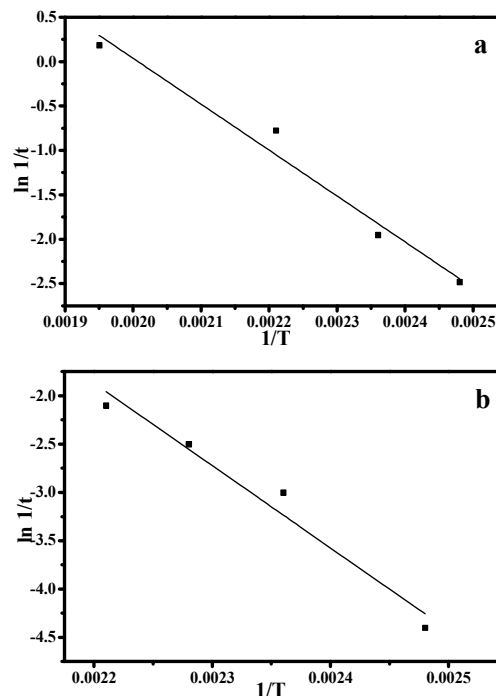


**Figure 5** Arrhenius plots for synthesizing RTH zeolite using (a) 2,6-methyl-N-methylpyridinium cation and (b) 1,2,3-trimethylimidazolium cation as organic templates.

literature. For example, Hong *et al.*<sup>6c</sup> use 1,2,3-trimethylimidazolium as organic template to synthesize RTH zeolite, giving the crystallization time for 16 days; Zones *et al.*<sup>5</sup> employ polymethylated [4.1.1] octanes to synthesize zeolite SSZ-50 with the crystallization time of 5-6 days. When increasing the crystallization temperature to 180 °C and even to 240 °C, we have still managed to produce RTH zeolites while significantly shortening the crystallization time (3 h at 180 °C and 50 min at 240 °C, Run 15-16, Table 2, Figure 4).

Figure S4 shows the changes of the crystalline phases during the crystallization of RTH zeolite at 130 °C. After 6 h crystallization time, the sample still shows peaks associated with Y zeolite (Figure S4A-b). The typical morphology assigned to Y zeolite is clearly observed *via* SEM image (Figure S4B-b). After 9 h crystallization time, the sample (Figure S4A-c) at 25° (2 theta) shows peaks associated with RTH zeolite structure. At the same time, block-like crystals appear in the product zeolites (Figure S4B-c), indicating the formation of RTH zeolite. Increasing the crystallization time from 10 to 11 h, the intensity of XRD peaks associated to RTH phase gradually increases (Figure S4A-d-e). Correspondingly, more RTH zeolite crystals are

## Journal Name

## ARTICLE

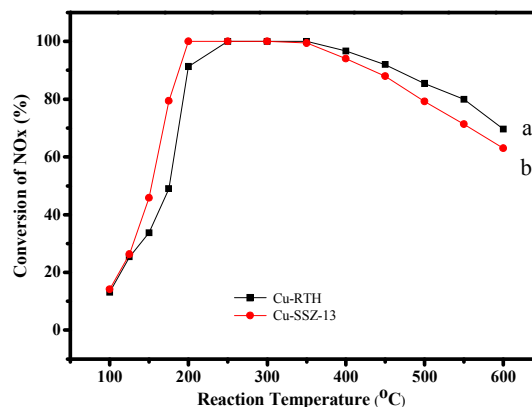
formed in the products (Figure S4B-d-e). RTH zeolite with high crystallinity can be obtained after a crystallization of 12 h (Figure S4A-f). Further increasing the crystallization time to 432 h, the intensity of XRD peaks show no change, which means the formed RTH phase is stable under these synthesis conditions.

Figure 4 and Figure S5 show the dependences of RTH zeolite crystallinity on crystallization time using 2,6-methyl-N-methylpyridinium cation and 1,2,3-trimethylimidazolium cation as OSDAs under different crystallization temperatures, respectively. From Arrhenius plots depicted in Figure 5, the activation energy using 2,6-methyl-N-methylpyridinium cation and 1,2,3-trimethylimidazolium cation is 42.0 kJ/mol and 70.8 kJ/mol, respectively. Obviously, lower activation energy is more favorable for rapid synthesis of RTH zeolite. In addition, the same zeolite building units of four-membered rings (4MRs) in both Y and RTH zeolite frameworks and higher framework density of RTH than that of Y zeolite might be helpful for the successful transformation from Y zeolite to RTH zeolite.<sup>9-11</sup>

Figure S6 shows the XRD patterns of as-synthesized RTH zeolite and RTH zeolites calcined at 550 °C, 700 °C and 850 °C for 4 h, respectively. When calcination temperature is below 700 °C, the RTH zeolite has good stability. When RTH zeolite is calcined at 850 °C, the crystallinity of the RTH zeolite reduced remarkably. Figure S7A and S7B show the <sup>29</sup>Si and <sup>27</sup>Al MAS NMR spectra of H-RTH zeolites calcined at 550 °C, 700 °C and 850 °C, respectively. The peak at -105.3 ppm in Figure S7A is assigned to Si(3Si)OH species, giving at 2.7%, 3.1% and 3.8% in the total <sup>29</sup>Si peak area of the samples calcined at 550 °C, 700 °C and 850 °C, respectively. These results suggest that the RTH zeolites calcined at higher temperature have higher concentration of structural defects (Si-OH), which should decrease the thermal stability of the RTH zeolite structure. The signals around 0 ppm in Figure S7B is associated with extraframework Al species, showing positive effect to the calcination temperature. These results indicate severe dealumination of RTH zeolite at high calcination temperature.

Figure S8 shows NH<sub>3</sub>-TPD curves of H-RTHs calcined at 550 °C, 700 °C and 850 °C, respectively. Obviously, the sample calcined at lower temperature has more acidic sites than that of calcined at higher temperature. The BET surface areas and micropore volume of these samples are presented in Table S1. It is clear that the surface areas and micropore volume of the samples calcined at 550 °C and 700 °C are very similar. However, when increasing the calcination temperature to 850 °C, both BET surface area and micropore volume decrease greatly, in according with those obtained from XRD patterns.

Figure 6 shows the dependence of the NO<sub>x</sub> conversion as a function of the reaction temperatures ranged from 100 to 600 °C in



**Figure 6** NO<sub>x</sub> conversion as a function of temperature in NH<sub>3</sub>-SCR over (a) Cu-RTH synthesized at 130 °C and (b) Cu-SSZ-13 obtained from BASF.

the NH<sub>3</sub>-SCR over the Cu-RTH catalyst synthesized at 130 °C and a Cu-SSZ-13 catalyst provided by BASF. Notably, the Cu-RTH catalyst exhibits promising catalytic performance (above 90% of NO conversion in the temperature range of 200–450 °C, Figure 6a), which is completely comparable with those of Cu-SSZ-13 catalyst (Figure 6b).

#### Catalytic tests

Figure 7 shows catalytic activities in MTO reactions over H-RTH and H-ZSM-5 catalysts as function of time on stream at 480 °C. The weight hourly space velocity (WHSV) is 1.0 h<sup>-1</sup>. Table 3 presents the results of the MTO reactions for a reaction time of 90 min at 480 °C. Obviously, compared with the H-ZSM-5 catalyst, H-RTH catalyst gives very high selectivity for ethylene and propylene (> 75%), which is very important for selective production of light olefins in the industrial processes. Figure S9 shows catalytic data in MTO reactions over H-RTH and H-ZSM-5 catalyst under different reaction temperature and weight hourly space velocity (WHSV). The results show that decreasing the reaction temperature could enhance the catalyst life, while decrease the selectivity for ethylene and propylene. In contrast, increasing the WHSV results in reduction of catalyst life and the selectivity for ethylene and propylene, compared with those in Figure 7.

Compared to catalytic data in the literatures, the selectivity for ethylene and propylene in the H-RTH catalyst (76.8%, Si/Al ratio at 8.8) in this work is higher than that of the H-RTH with Si/Al at 17 (64%)<sup>6a</sup> and the H-RTH catalyst with B species (73.3%).<sup>7</sup> The

**Table 3** The results of MTO reactions for a reaction time of 90 minutes at 753 K.

|         | SiO <sub>2</sub> / Al <sub>2</sub> O <sub>3</sub> | Conv. [%] | Selectivities (%)             |                               |   |                  |
|---------|---|-----------|-------------------------------|-------------------------------|---|------------------|
|         |   |           | C <sub>2</sub> H <sub>4</sub> | C <sub>3</sub> H <sub>6</sub> | C <sub>2</sub> H <sub>4</sub> + C <sub>3</sub> H <sub>6</sub> | ≥ C <sub>4</sub> |
| H-RTH   | 17.6  | 100       | 40.5                          | 36.3                          | 76.8  | 12.2             |
| H-ZSM-5 | 20.8  | 100       | 26.0                          | 19.9                          | 45.9  | 38.3             |

difference in the catalytic selectivity might be resulted from their distinguishable composition in the RTH zeolite.

## Conclusions

In summary, we have employed a novel organic template (2,6-methyl-N-methylpyridinium) for synthesizing aluminosilicate zeolite RTH. The crystallization of RTH is very fast (12 h at 130 °C and 50 min at 240 °C). Theoretical calculations have confirmed that this template is more suitably matched with the RTH pore geometry than other conventional organic templates. More importantly, catalytic tests in NH<sub>3</sub>-SCR and MTO reactions show that the Cu-RTH and H-RTH are promising catalysts for these transformation. The combination of rapid crystallization and excellent catalytic properties might offer a good opportunity for wide applications of RTH zeolites in the near future.

## Author contribution

X. Hao and S. X. Pan performed the zeolite catalysts. L. Zhang and C. S. Zhang performed catalytic tests. Y. Y. Chu performed the theoretical calculations. R. McGuire, A. N. Parvulescu and U. Müller partially discussed and analyzed results for synthesis and catalysis. J. G. Jiang and F. Deng partially discussed and analyzed the results of NMR data. L. F. Zhu, X. J. Meng and S. Maurer partially discussed and analyzed the catalytic results. Q. M. Wu and F.-S. Xiao designed this study, analyzed the data, and wrote the paper.

## Conflicts of interest

There are no conflicts of interest to declare.

## Acknowledgements

This work is supported by National Key Research and Development Program of China (2017YFC0211101), National Natural Science Foundation of China (21333009, 21703203 and 21673205), China Postdoctoral Science Foundation (2017M611978).

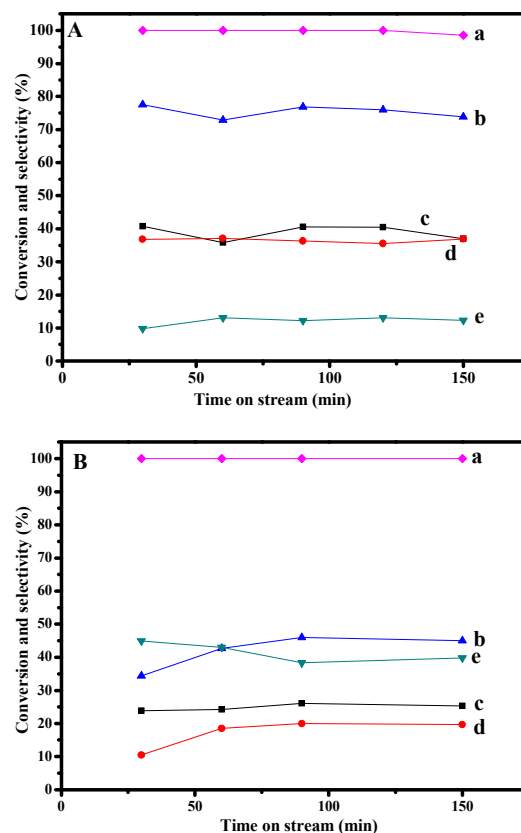


**Figure 7** (a) Methanol conversion (◆) and product selectivities of (b) ethylene with propylene (▲C<sub>2</sub>H<sub>4</sub> + C<sub>3</sub>H<sub>6</sub>), (c) ethylene (■C<sub>2</sub>H<sub>4</sub>), (d) propylene (●C<sub>3</sub>H<sub>6</sub>) and (e) hydrocarbons higher than C<sub>4</sub> (▼≥C<sub>4</sub>) in MTO over (A) H-RTH and (B) H-ZSM-5 catalysts.

## References

- (a) M. E. Davis, R. F. Lobo, *Chem. Mater.*, 1992, **4**, 756; (b) H. Gies, B. Marler, *Zeolite*, 1992, **12**, 42; (c) C. S. Cundy, P. A. Cox, *Chem. Rev.*, 2003, **103**, 663; (d) K. Moller, T. Bein, *Chem. Soc. Rev.*, 2013, **42**, 3689; (e) S. Mintova, J. P. Gilson, V. Valtchev, *Nanoscale*, 2013, **5**, 6693; (f) M. E. Davis, *Chem. Mater.*, 2014, **26**, 239; (g) M. Moliner, C. Martínez, A. Corma, *Chem. Mater.*, 2014, **26**, 246; (h) X. J. Meng, F.-S. Xiao, *Chem. Rev.*, 2014, **114**, 1521.
- (a) J. Scherzer, *Appl. Catal.*, 1991, **75**, 1; (b) B. Xu, S. Bordiga, R. Prins, J. A. van Bokhoven, *Appl. Catal. A: Gen.*, 2007, **333**, 245; (c) P. T. M. Do, J. R. McAtee, D. A. Watson, R. F. Lobo, *ACS Catal.*, 2013, **3**, 41; (d) Z. Qin, B. Shen, Z. Yu, F. Deng, L. Zhao, S. Zhou, D. Yuan, X. Gao, B. Wang, H. Zhao, H. Liu, *J. Catal.*, 2013, **298**, 102; (e) J. Cejka, B. Wichterlova, *Catal. Rev.*, 2002, **44**, 375; (f) S. R. Zheng, A. Jentys, J. A. Lercher, *J. Catal.*, 2006, **241**, 304; (g) R. J. Balasamy, T. Odedairo, S. Al-Khattaf, *Appl. Catal. A: Gen.*, 2011, **409**, 223.
- (a) Q. Zhu, J. N. Kondo, T. Tatsumi, S. Inagaki, R. Ohnuma, Y. Kubota, Y. Shimodaira, H. Kobayashi, K. Domen, *J. Phys. Chem. C*, 2007, **111**, 5409; (b) U. Olsbye, S. Svelle, M. Bjørgen, P. Beato, T. V. W. Janssens, F. Joensen, S. Bordiga, K. P. Lillerud, *Angew. Chem. Int. Ed.*, 2012, **51**, 5810; (c) N. Martin, M. Moliner, A. Corma, *Chem. Commun.*, 2015, **51**, 9965; (d) Z. Li, M. Navarro, J. Martínez-Triguero, J. Yu, A. Corma, *Catal. Sci. Technol.*, 2016, **6**, 5856; (e) P. Tian, Y. Wei, M. Ye, Z. Liu, *ACS Catal.*, 2015, **5**, 1; (f) L. Xie, F. Liu, X. Shi, F. Xiao, H. He, *Appl. Catal. B: Environ.*, 2015,

## ARTICLE

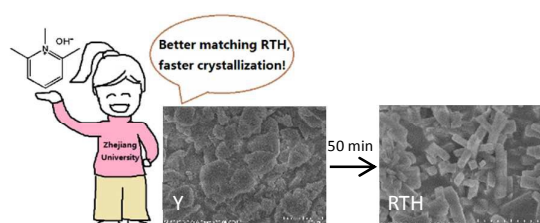
Journal Name

- 179, 206; (g) L. Wu, V. Degirmenci, P. C. M. M. Magusin, B. M. Szyja, E. J. M. Hensen, *Chem. Commun.*, 2012, **48**, 9492; (h) F. Gao, E. D. Walter, E. M. Karp, J. Luo, R. G. Tonkyn, J. H. Kwak, J. Szanyi, C. H. F. Peden, *J. Catal.*, 2013, **300**, 20; (i) D. W. Fickel, R. F. Lobo, *J. Phys. Chem. C*, 2010, **114**, 1633.
4. S. Vortmann, B. Marler, H. Gies, P. Daniels, *Microporous Mater.*, 1995, **4**, 111.
  5. G. Lee, S. Zones, *J. Solid State Chem.*, 2002, **167**, 289.
  6. (a) J. E. Schmidt, M. A. Deimund, M. E. Davis, *Chem. Mater.*, 2014, **26**, 7099; (b) J. E. Schmidt, M. A. Deimund, D. Xie, M. E. Davis, *Chem. Mater.*, 2015, **27**, 3756; (c) D. Jo, J. Bin Lim, T. Ryu, I. S. Nam, M. A. Cambor, S. B. Hong, *J. Mater. Chem. A*, 2015, **3**, 19322.
  7. T. Yokoi, M. Yoshioka, H. Imai, T. Tatsumi, *Angew. Chem. Int. Ed.*, 2009, **48**, 9884.
  8. L. F. Zhu, L. M. Ren, S. J. Zeng, C. G. Yang, H. Y. Zhang, X. J. Meng, M. Rigutto, A. van der Made, F.-S. Xiao, *Chem. Commun.*, 2013, **49**, 10495.
  9. K. Honda, M. Itakura, Y. Matsuura, A. Onda, Y. Ide, M. Sadakane, T. Sano, *J. Nanosci. Nanotechnol.*, 2013, **13**, 3020.
  10. S. Goel, S. I. Zones, E. Iglesia, *Chem. Mater.*, 2015, **27**, 2056.
  11. B. N. Bhadra, P. W. Seo, N. A. Khan, J. W. Jun, T. Kim, C. Kim, S. H. Jung, *Catal. Today*, 2017, **298**, 53.

## Table of contents

### Efficient synthesis of aluminosilicate RTH zeolite with good catalytic performances in $\text{NH}_3$ -SCR and MTO reactions

Hao Xu, Qinming Wu,\* Yueying Chu, Jingang Jiang, Ling Zhang, Shuxiang Pan, Changsheng Zhang, Longfeng Zhu, Feng Deng, Xiangju Meng, Stefan Maurer, Robert McGuire, Andrei-Nicolae Parvulescu, Ulrich Müller and Feng-Shou Xiao\*



The synthesis of aluminosilicate RTH zeolite is very fast in the presence of 2,6-methyl-N-methylpyridinium cation.